Particle Transport Due to Magnetic Fluctuations

M. R. Stoneking, S. A. Hokin, S. C. Prager, G. Fiksel, H. Ji, and D. J. Den Hartog
Department of Physics, University of Wisconsin, Madison, Wisconsin 53706
(Received 13 January 1994)

Electron current fluctuations are measured with an electrostatic energy analyzer at the edge of the MST reversed-field pinch plasma. The radial flux of fast electrons ($E > T_{ea}$) due to parallel streaming along a fluctuating magnetic field is determined locally by measuring the correlated product $\langle \tilde{J}_e \tilde{B}_r \rangle$. Particle transport is small just inside the last closed flux surface ($\Gamma_{e,\mathrm{mag}} < 0.1\Gamma_{e,\mathrm{total}}$), but can account for all observed particle losses inside $r/a = 0.85$. Electron diffusion is found to increase with parallel velocity, as expected for diffusion in a region of field stochasticity.

PACS numbers: 52.55.Hc, 52.25.Fi, 52.35.Ra

Plasma transport across a confining magnetic field continues to be a central problem in the field of plasma physics, engendering numerous experimental, theoretical, and computational studies. The mechanisms responsible for fluctuation induced transport are broadly classified as either electrostatic or magnetic in origin. For example, radial electron particle flux can be described by [1]

$$\Gamma_{r,e} = \frac{\langle \tilde{n}\tilde{E}_\perp \rangle}{B} - \frac{\langle \tilde{J}_{\parallel,e}\tilde{B}_r \rangle}{eB}, \qquad (1)$$

where the symbol $\langle \tilde{a}\tilde{b} \rangle$ indicates the flux surface averaged product of the fluctuating quantities (density $\tilde{n}$, perpendicular electric field $\tilde{E}_\perp$, parallel electron current $\tilde{J}_{\parallel,e}$, and radial magnetic field $\tilde{B}_r$), and B is the magnitude of the confining field. The first term in Eq. (1) represents the electrostatic contribution to the flux and results from the fluctuating $\tilde{\boldsymbol{E}} \times \boldsymbol{B}$ guiding center drift. The second term describes the magnetic transport due to fluctuations in the parallel streaming electron flux which are correlated and in phase with fluctuations in B_r. Measurements of the local *electrostatic* transport have been obtained in the octupole [2], the tokamak [3], the stellarator [4], and the reversed-field pinch [5–7]. However, transport due to *magnetic* fluctuations has been mainly studied indirectly by measuring runaway electron flux to a limiter [8–10]. Such experiments are useful for probing the magnetic fluctuations, but do not provide a local measurement of particle transport resulting from $\tilde{B}$. Magnetic transport is expected to contribute significantly to energy loss in a plasma with magnetic fluctuations [11,12]. Under certain conditions particle transport due to magnetic turbulence is expected to be ambipolar [13], and recent measurements of the ambipolarity of magnetic fluctuation induced transport at the edge of a reversed-field pinch support the theoretical conclusions [14]. However, the magnitude of the ambipolar flux driven by magnetic fluctuations has not been directly measured previously.

In this Letter we report on local measurements of $\langle \tilde{J}_{\parallel,e}\tilde{B}_r \rangle$, the electron particle transport due to magnetic fluctuations in the outer region ($r/a > 0.75$) of the Madison Symmetric Torus (MST) plasma, employing an electrostatic electron energy analyzer (EEA) which incorporates a magnetic coil triplet. The outward electron particle flux just inside the last closed flux surface (LCFS) is small due to weak correlation of the fluctuations. The transported flux increases to the level of the total particle losses inside $r/a = 0.85$ where integrity of the magnetic flux surfaces is believed to be destroyed.

MST [15,16] is a reversed-field pinch (RFP) toroidal confinement device [17]. The level of magnetic turbulence in the RFP is higher than in the tokamak, and thus provides a suitable environment for studying magnetic transport phenomena. MST has a major radius of 1.5 m and minor radius of 0.51 m. Probe data are obtained at $r/a > 0.9$ in discharges of 50 ms duration and toroidal plasma current, $I_\phi = 210$ kA. Low current discharges ($I_\phi = 120$ kA) with similar field profiles and confinement properties are used to obtain transport measurements in to $r/a = 0.75$ without significant perturbation of the global plasma signals. The central electron temperature is typically 100 eV, and global particle and energy confinement times are approximately 1 ms.

The electron current is measured using a two-channel EEA [18] with one channel aligned with the local magnetic field in each direction. A schematic diagram of the analyzer is shown in Fig. 1. A channel consists of three electrodes: an entrance aperture 0.3 mm in diameter that eliminates ion current (typical ion gyro-orbits have radii $\rho_i = 1$ cm), a cylindrical "repeller" electrode that determines the minimum electron energy accepted, and an

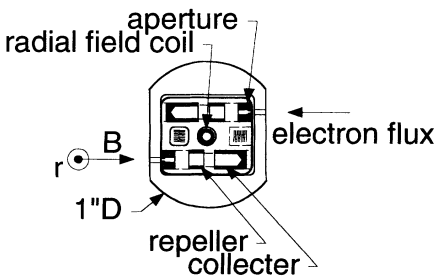

FIG. 1. Schematic of the electron energy analyzer.

0031-9007/94/73(4)/549(4)$06.00

electron current collector. The entrance electrode and the collector were maintained at machine ground potential and the repeller electrode was biased to -50V, suppressing the loss of secondary electrons from the collector. Data presented here represent the behavior of the energetic (and nearly collisionless $\lambda_{mfp} \approx 10$ m) component of the distribution which has a parallel (effective) temperature comparable to the central electron temperature $T_{\|} \approx 100$ eV. The two channels are offset by 0.8 cm perpendicular to the field and the signals from the two channels are ~60% correlated at low frequency. The modest decorrelation results from the short perpendicular correlation length (~5 cm) of the electron current fluctuations and the collisionless or ballistic nature of the detected particles, which are presumably accelerated in a region distant from the measurement site. The equilibrium fast electron current is recovered by taking the difference of the averaged signals from the two EEA channels. The asymmetry in the electron current detected by the two channels varies from $J_+/J_- = 2$ to 5 depending on the plasma density (where electron current J_+ is in the direction required to carry the equilibrium current), but the net equilibrium current obtained after calibration agrees with measurements of the total parallel current measured with insertable magnetic probes (e.g., Rogowski probe) independent of density (qualitatively similar results were found in other RFP experiments, see, for example, Ref. [18]). This is taken as evidence that the local perturbation to the fast electron population due to the probe is not significant. The angular acceptance of the aperture is 11° (full width) compared to the 1°–2° deflections in the magnetic field direction due to turbulent fluctuations ensuring collection of electrons streaming along the fluctuating field during all phases of the fluctuation; cross-field drift velocities are negligible compared to the parallel streaming velocity ($v_{\|} \approx 4 \times 10^6$ m/s) ensuring that the current is parallel to the local field. Electron current and magnetic field measurements are made at the same radial position. Records used in statistical ensembles are taken at a time just after peak plasma current, and sampled at 500 kHz. More than one hundred 1 ms records are used in each ensemble average taken from 25 to 50 nominally identical discharges. Typical electron current (J_+) and radial sense coil signals for the times of interest are shown in Fig. 2. The rms fluctuation amplitude in the electron current is close to 100%; the magnetic fluctuation amplitude is 2%. The extremely localized nature of the electron current measurement makes it sensitive to fluctuations at small spatial scales and the high fluctuation amplitude indicates the filamentary character of the electron current.

The frequency spectrum of electron current fluctuations ($\tilde{J}_+$) is featureless and falls off more slowly than the $\tilde{B}$ spectrum at high frequency (Fig. 3), as expected from $\tilde{\boldsymbol{J}} = i\boldsymbol{k} \times \tilde{\boldsymbol{B}}$ if $\boldsymbol{k}$ increases with frequency (the $\tilde{B}_\phi$ and $\tilde{B}_\theta$ power spectra fall off with a power law dependence as $f^{-5/2}$ at high frequency, while the $\tilde{B}_r$ spectum is closer to the $f^{-3/2}$ prediction from magnetohydrodynamics turbulence theory [19]). The backflow fluctuations ($\tilde{J}_-$) are 180° out of phase with the forward flow fluctuations, but are lower by roughly a factor of 10 in power. The dominant feature in the magnetic frequency spectra at low frequencies ($f < 10$ kHz) is due to current fluctuations resonant at low order mode rational surfaces in the plasma core (i.e., tearing modes) [20]. It is reasonable to assume that fast electron current fluctuations dominate the total current fluctuations. The fluctuation power in the electron current is then inferred to be dominated by local, short wavelength turbulence even at low frequency (through Ampere's law). This result is qualitatively consistent with the observation that the current fluctuation amplitude measured with magnetic probes that sample a ~1 cm diam area is 20%–40% rather than ~100% seen with the more localized EEA measurement. A more precise comparison of the relationship between the measured magnetic fluctuations and electron current fluctuations requires knowledge of the spatial structure of the current fluctuations that is not available.

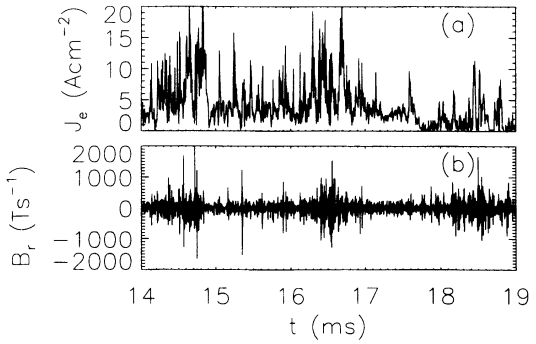

FIG. 2. Typical signals from the EEA during times of interest for discharges with $I_\phi = 210$ kA: (a) fast electron current in electron flow direction ($\tilde{J}_+$), (b) radial sense coil signal ($\dot{B}_r$).

Figure 4 shows the coherence and relative phase between electron current fluctuations ($\tilde{J}_+$) and radial magnetic field fluctuations just inside the LCFS ($r/a = 0.97$) for $I_\phi = 210$ kA. Coherence and relative phase are

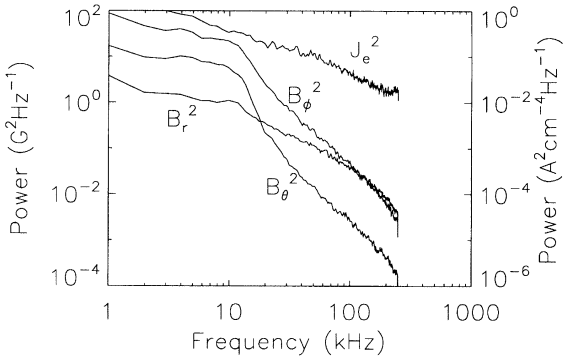

FIG. 3. The frequency power spectra of electron current ($\tilde{J}_+$) and magnetic field fluctuations.

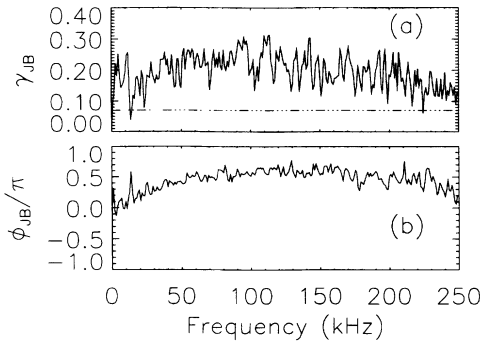

FIG. 4. (a) The coherence spectrum for electron current ($\tilde{J}_+$) and radial magnetic field fluctuations just inside the LCFS. The dashed line indicates the statistical confidence level. (b) The relative phase of the electron current and radial field fluctuations.

determined from the cross-power and fluctuation amplitudes by

$$\gamma_{ab} = \frac{|\langle \tilde{a}^* \tilde{b} \rangle|}{|\tilde{a}||\tilde{b}|}, \qquad \phi_{ab} = \arctan \frac{\mathrm{Im}\langle \tilde{a}^* \tilde{b} \rangle}{\mathrm{Re}\langle \tilde{a}^* \tilde{b} \rangle},$$

where the flux surface average for propagating fluctuations, $\langle \tilde{a}^* \tilde{b} \rangle$, is realized by making an ensemble average over many time records. The relation between the coherence, phase, fluctuation amplitudes, and the transported flux of electrons is

$$\Gamma_{r,e} = \frac{-1}{eB} \sum_{\omega} |\tilde{J}_e(\omega)||\tilde{B}_r(\omega)|\gamma_{JB}(\omega)\cos[\phi_{JB}(\omega)] \quad (2)$$

The coherence is 20% and the phase varies smoothly from zero to $\pi/2$ rad across the low frequency band where the fluctuation power is concentrated. The coherence is above the statistical confidence level determined by the number of records in the ensemble ($1/\sqrt{N} = 7\%$). The low coherence between the electron current fluctuations and the magnetic fluctuations at low frequency supports the inference made above that the electron current fluctuations are dominantly localized fluctuations (~80%) whereas the low frequency magnetic fluctuations are known to be global in character. The resulting radial particle flux, calculated from Eq. (2) and combined for the forward and "backflowing" signals, is $\Gamma_r < 5 \times 10^{20}\ \mathrm{m^{-2}\,s^{-1}}$. Estimates of the total radial electron particle flux from H_α emission profiles are $\Gamma_r \approx 5 \times 10^{21}\ \mathrm{m^{-2}\,s^{-1}}$. Magnetic fluctuation induced electron transport is thus a negligible ($\Gamma_{e,\mathrm{mag}} < 0.1\Gamma_{e,\mathrm{total}}$) channel for particle loss at the edge of the plasma. The ambipolarity of magnetic transport previously measured in MST [14] coupled with the results presented in this Letter imply that the ion particle transport due to magnetic fluctuations is also negligible near the LCFS. Local electron current fluctuations at the edge, while large, are not coherent with the dominant low frequency magnetic fluctuations in the core. The small transport resulting from the magnetic fluctuations implies significantly reduced field line diffusion at the edge of the RFP if the heuristic picture of transport due to streaming along a stochastic field is a valid one. The electrostatic transport of particles at $r/a = 0.97$ is larger than the edge magnetic particle transport by an order of magnitude, and is comparable to the total expected particle flux [6]. Similar results for electrostatic transport were obtained in the ZT-40M experiment [5].

Figure 5 shows that magnetic fluctuation induced electron transport increases with distance into the plasma. Measurements at deep insertion were made in low current ($I_\phi = 120$ kA) discharges. The transported flux reaches levels of the order of the total expected particle flux, while measured electrostatic particle transport falls off in this region. The increased transport is due to larger fluctuation amplitudes, rather than a rise in coherence or change in the relative phase between $\tilde{J}_e$ and $\tilde{B}_r$. Because the fluctuation amplitudes are peaked at low frequency, but the coherence is roughly constant across the bandwidth, the transport is dominated by the low frequency correlation (although weak). The authors interpret this result as implying that the global tearing instabilities lead to stochasticization of the field and are responsible for the transport. Only 20% of the measured current fluctuations are global in character and it is this component that contributes to the transport. Expected total particle flux (dashed lines) is found from a transport code and is consistent with the measured density profile and edge neutral pressure. The uncertainty in the total flux is primarily due to the uncertainty in the edge pressure. Measurements of magnetic particle transport at the edge (circles in Fig. 5) were made in $I_\phi = 210$ kA discharges and have been normalized to the same line averaged plasma density as the low current case. The profiles match in the region of overlap consistent with the observation that global confinement is comparable for the two cases.

Our measurements indicate that magnetic fluctuation induced transport of fast electrons can account for the

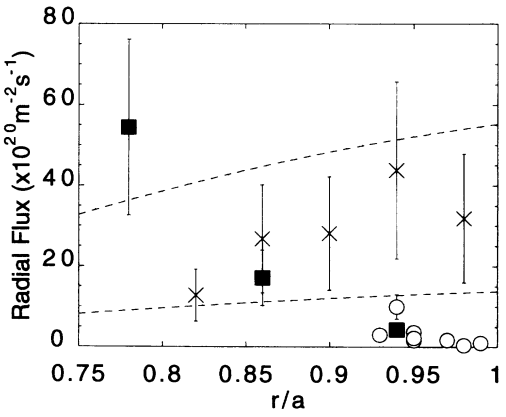

FIG. 5. The radial profiles of transported electron flux due to magnetic fluctuations (■), the electrostatic particle flux (×), and the range of expected total particle flux (dashed lines) for $I_\phi = 120$ kA. Edge measurements of magnetic transport of electrons (○) at $I_\phi = 210$ kA have been normalized to the same plasma density as the 120 kA case.

expected total electron flux inside $r/a = 0.85$. These results are consistent with the conclusions of confinement scaling measurements done on the Extrap-T1 RFP [21]. The fast electron diffusion coefficient, obtained by dividing $\Gamma_{e,\mathrm{fast}}$ into $\nabla n_{e,\mathrm{fast}}$, is $D_{\mathrm{fast}} \approx 500 \pm 250\ \mathrm{m}^2/\mathrm{s}$. If electron transport were unconstrained by ambipolar considerations, collisionless diffusion in a region of field stochasticity would proceed at a rate given by [12]

$$D = \frac{\langle \tilde{B}_r^2 \rangle}{B_0^2} v_{\mathrm{av}} L_{\mathrm{ac}}, \tag{3}$$

where v_{av} is the average fast electron parallel velocity and L_{ac} is the parallel autocorrelation length for the magnetic fluctuations. L_{ac} is determined from the magnetic wave number spectra $L_{\mathrm{ac}} = \pi/\Delta k_{\|} \approx 1$ m (the fast electrons are collisionless since their mean free path is about 10 m). For the discharge conditions discussed here and $T_{e,\mathrm{fast}} = 100$ eV, Eq. (3) predicts $D = 2000\ \mathrm{m}^2/\mathrm{s}$, 4 times the observed fast electron diffusion rate of $500\ \mathrm{m}^2/\mathrm{s}$. It is very difficult to reconcile the measured diffusion with the naive application of Eq. (3). All the numbers entering into Eq. (3) are accurately known, although the model is admittedly heuristic.

If the stochastic diffusion mechanism described by Eq. (3) is active, a radial ambipolar electric field will be established by the rapid transport of highly mobile electrons. The ambipolar field then inhibits further electron transport. The magnitude of the ambipolar electric field required to suppress electron transport in a stochastic field is given by [22]

$$E_A = -\frac{T_e}{e}\left(\frac{\nabla n}{n} + \frac{\nabla T_e}{2T_e}\right). \tag{4}$$

For the plasma conditions of interest in this Letter, E_A is approximately 500 V/m. The $\boldsymbol{E} \times \boldsymbol{B}$ flow induced by the ambipolar field is comparable in magnitude and in the same direction as the ion diamagnetic drift. The expected flow is in qualitative agreement with the measured toroidal rotation speed (10^6 cm/s $\approx v_{\boldsymbol{E}\times\boldsymbol{B}} + v_{Di}$) of C^{+4} impurity ions [23] as well as the toroidal propagation speed of the tearing modes [24]. In the presence of a radial ambipolar electric field, stochastic diffusion proceeds at the rate given by Eq. (3), using the *ion* thermal velocity, i.e., the ion stochastic diffusion rate. For the relevant plasma conditions, the ion stochastic diffusion coefficient is about $50\ \mathrm{m}^2/\mathrm{s}$. Global particle balance inferred from H_α emission and equilibrium plasma density profiles also requires an ambipolar diffusion coefficient of $50\ \mathrm{m}^2/\mathrm{s}$. The fast electron diffusion proceeds at $500\ \mathrm{m}^2/\mathrm{s}$ because the fast electron density is roughly 10% of the bulk plasma density. Bulk electron transport is entirely suppressed by the ambipolar field.

Information about the energy dependence of magnetic particle transport is obtained by changing the bias potential on the repeller electrode of the EEA. The radial flux of electrons is observed to decrease more slowly than the parallel electron current with increasing repeller bias, indicating that higher energy electrons are preferentially transported by magnetic fluctuations, consistent with a stochastic transport mechanism [Eq. (3)].

In summary, we have measured for the first time the local electron particle flux produced by magnetic fluctuations. Measurements in MST show that magnetic fluctuation induced particle transport dominates the core of the RFP plasma. Recent measurements of the energy transport due to magnetic fluctuations in MST [25] display the same radial dependence as the particle transport and the magnitude is consistent with the convective energy carried by the fast electron particle flux reported in this Letter. Numerical simulations of the RFP plasma indicate that magnetic flux surfaces are destroyed in the core [26] consistent with our observation of large and increasing radial particle flux due to magnetic transport as the core is approached. Additionally, electron transport is found to be dominated by the high energy component of the distribution.

The authors are grateful for physics discussion with Dr. W. Shen and the members of the MST group. This work was supported by the U.S. Department of Energy.

[1] P. C. Liewer, Nucl. Fusion **25**, 543 (1985).
[2] J. A. Schmidt, Phys. Rev. Lett. **24**, 721 (1970).
[3] W. L. Rowan *et al.*, Nucl. Fusion **27**, 1105 (1987).
[4] T. Uckan *et al.*, J. Nucl. Mater. **176–177**, 693 (1990).
[5] P. G. Weber *et al.*, in *Proceedings of the International Conference on Plasma Physics and Controlled Nuclear Fusion Research* (IAEA, Washington, D.C., 1990), Vol. 2, p. 509.
[6] T. D. Rempel *et al.*, Phys. Rev. Lett. **67**, 1438 (1991).
[7] H. Ji *et al.*, Phys. Rev. Lett. **67**, 62 (1991).
[8] C. W. Barnes and J. D. Strachan, Nucl. Fusion **22**, 1090 (1982).
[9] C. W. Barnes and J. D. Strachan, Phys. Fluids **26**, 2668 (1983).
[10] P. J. Catto *et al.*, Phys. Fluids B **3**, 2038 (1991).
[11] J. D. Callen, Phys. Rev. Lett. **39**, 1540 (1977).
[12] A. B. Rechester and M. N. Rosenbluth, Phys. Rev. Lett. **40**, 38 (1978).
[13] R. E. Waltz, Phys. Fluids **25**, 1269 (1982).
[14] W. Shen *et al.*, Phys. Rev. Lett. **68**, 1319 (1992).
[15] R. N. Dexter *et al.*, Fusion Tech. **19**, 131 (1991).
[16] S. Hokin *et al.*, J. Fusion Energy **12**, 281 (1993).
[17] H. A. B. Bodin and A. A. Newton, Nucl. Fusion **19**, 1255 (1980).
[18] J. C. Ingraham *et al.*, Phys. Fluids B **2**, 143 (1990).
[19] R. H. Kraichnan, Phys. Fluids **8**, 1385 (1965).
[20] G. Chartas and S. Hokin, Phys. Fluids B **4**, 4019 (1992).
[21] S. Mazur *et al.*, Phys. Rev. E **48**, R680 (1993).
[22] R. W. Harvey *et al.*, Phys. Rev. Lett. **47**, 102 (1981).
[23] D. J. Den Hartog *et al.*, Bull. Am. Phys. Soc. **38**, 1979 (1993), *abstract only*.
[24] A. F. Almagri *et al.*, Phys. Fluids B **4**, 4080 (1992).
[25] G. Fiksel *et al.*, Phys. Rev. Lett. **72**, 1028 (1994).
[26] D. D. Schnack, E. J. Caramana, and R. A. Nebel, Phys. Fluids **28**, 321 (1985).

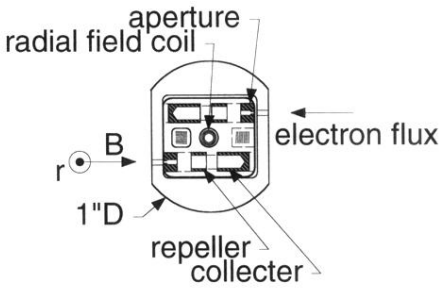

FIG. 1. Schematic of the electron energy analyzer.